Makara Journal of Science

Volume 28
Issue 3 *September*

Article 4

9-27-2024

Immobilization of Ni(II) on Amine-Functionalized Mesoporous Silica as Catalyst for Benzyl Alcohol Acetylation Reaction

Wardah Nabilah
Department of Chemistry, Universitas Gadjah Mada, Yogyakarta 55281, Indonesia

Eko Sri Kunarti
Department of Chemistry, Universitas Gadjah Mada, Yogyakarta 55281, Indonesia,
eko_kunarti@ugm.ac.id

Fajar Inggit Pambudi
Department of Chemistry, Universitas Gadjah Mada, Yogyakarta 55281, Indonesia

Makara Journal of Science, 28/3 (2024), 209-215
doi: 10.7454/mss.v28i3.2216

Immobilization of Ni(II) on Amine-Functionalized Mesoporous Silica as Catalyst for Benzyl Alcohol Acetylation Reaction

Wardah Nabilah, Eko Sri Kunarti*, and Fajar Inggit Pambudi

Department of Chemistry, Universitas Gadjah Mada, Yogyakarta 55281, Indonesia

*E-mail: eko_kunarti@ugm.ac.id

Received September 7, 2023 | Accepted July 8, 2024

Abstract

In this study, amine-functionalized and Ni(II)-immobilized mesoporous silica materials were synthesized. This research aimed to synthesize mesoporous silica based on rice husk ash functionalized with amine and immobilized with Ni(II). The activity of amine-functionalized and Ni(II)-immobilized mesoporous silica materials was studied for the acetylation of benzyl alcohol with acetic anhydride as the acetylating agent. First, mesoporous silica was synthesized using rice husk ash using the sol–gel method, followed by amine functionalization using (3-aminopropyl)triethoxysilane (APTES) and Ni(II) immobilization through ultrasonic treatment. The results obtained showed that amine-functionalized and Ni(II)-immobilized mesoporous silica (SiO_2/APTES/Ni(II)) were successfully synthesized, confirmed by Fourier transform infrared and Energy-dispersive X-ray spectrometry data. In addition, the synthesized materials had an average pore diameter of 12.83 nm. Afterward, the catalytic activity test showed that SiO_2/APTES/Ni(II) was able to convert 98.34% of benzyl alcohol in the acetylation reaction at 45 °C for 5 h. The use of the SiO_2/APTES/Ni(II) catalyst for three cycles obtained percent conversion values with a slight decreases (98.34%, 95.20%, and 90.61%).

Keywords: acetylation, benzyl acetate, catalyst, mesoporous silica, SiO_2/APTES/Ni(II)

Introduction

Benzyl acetate, a carboxylic acid ester, finds common utility across diverse industries, including food and cosmetics, particularly in the formulation of perfumes and flavorings. Although this ester compound is found naturally in gardenia and jasmine plants, its purification and extraction present intricate challenges. Therefore, various methods have emerged for synthesizing benzyl acetate [1]. Conventionally, benzyl acetate synthesis involves the reaction between benzyl alcohol and acetic anhydride in the presence of sulfuric acid as a homogeneous catalyst. However, using sulfuric acid in synthesizing benzyl acetate is plagued by several drawbacks, such as the formation of unwanted by-products and the generation of environmentally detrimental waste materials [2]. Given these limitations, several transition metal ions such as In(III), Ga(III), Fe(III), Zn(II), Cu(II), Ni(II), and Co(II) have been widely used in esterification and have demonstrated promising catalytic efficacy [3].

The immobilization of a catalyst onto support materials boosts the advantages of heterogeneous systems, including facile production processes and the potential for catalyst recycling [4]. Solid heterogeneous catalysts with supporting materials such as clay [5], zeolite [6], alumina [7], and resin [8] are commonly used because of their unique catalytic properties and easy recycling. Among these, mesoporous silica is a favored support material because it has high stability and good interaction with both metal ions and metal nanoparticles. In this regard, Alam *et al*. [9] reported that Ni/SiO_2 as a catalyst in the acetylation of benzyl alcohol with acetic anhydride showed great activity by giving a 97% conversion yield after a 3.5 h reaction at 65 °C.

Silica can be procured through synthesis from precursors or by extraction from natural resources. Rice husk ash, characterized by a substantial SiO_2 content ranging from approximately 15% to 60%, represents one such natural source of silica [10]. For this reason, in this study, catalysts with mesoporous silica as a support material were synthesized using rice husk ash. Previous studies have shown that mesoporous silica as catalyst support has superior properties. However, there is one crucial drawback threatening to diminish catalyst reusability: metal leaching [11]. Thus, various binding agents, such as phosphine [12], imine [13], L-dopa [14], and amines [15], are known to provide strong interactions with metals to enhance the stability of catalyst materials by preventing the metal leaching tendency [15]. However, although some research has explored the use of silica derived from rice husk ash as a composite catalyst for organic reactions

[16, 17], the application of rice-husk-ash-derived mesoporous silica specifically for benzyl alcohol acetylation remains a relatively unexplored area. This study addresses this gap by investigating the catalytic activity of amine-functionalized and Ni(II)-immobilized mesoporous silica (SiO_2/APTES/Ni(II)) synthesized using rice husk ash and ultrasonic treatment. This approach offers a potentially sustainable and efficient catalyst for benzyl alcohol acetylation.

Materials and Methods

Materials and Characterization. Rice husk ash was obtained from SB Farm Semarang. The other materials of proanalytical quality were obtained from Sigma-Aldrich, such as hydrochloric acid (HCl; 37%), (3-aminopropyl)triethoxysilane ($C_9H_{23}NO_3Si$ [APTES]; 98%), sodium hydroxide (NaOH), ethanol (C_2H_5OH; 99,8%), PEG-40 hydrogenated castor oil, nickel(II) nitrate hexahydrate ($Ni(NO_3)_2{\cdot}6H_2O$), benzyl alcohol ($C_6H_5CH_2OH$), and acetic anhydride ($(CH_3CO)_2O$). The catalyst was characterized using an X-ray diffractometer (XRD-Bruker AXS D8 Advance Eco), a scanning electron microscope (SEM)–energy-dispersive X-ray spectrometer (JSM-6510LA), a Fourier transform infrared (FTIR) spectrometer (Thermo Scientific Nicolet iS10), a thermogravimetric analyzer (TGA; Perkin Elmer Pyris 1), and an X-ray fluorescence spectrometer (Rigaku-Nex QC + QuanTEZ). Then, the products yielded were analyzed using gas chromatography (GC; Agilent Technologies 7890B).

Synthesis of silica. Sodium silicate was synthesized through the alkaline extraction of 10 g of rice husk ash with 60 mL of 1 N NaOH [18] after acid treatment and calcination. In synthesizing mesoporous silica, 30 mL of Na-silicate was neutralized by hydrochloric acid until pH = 7. Then, PEG-40 hydrogenated castor oil with a concentration of 10% was added as a template and stirred until it formed a homogeneous mixture. Afterward, the mixture was sonicated for 1 h to obtain a gel phase and heated at 80 °C for 24 h. The template was then removed by adding ethanol 1:10 (m/v) into silica, followed by sonication for 1 h at room temperature. The mixture was subsequently filtered and washed using cold ethanol three times before being dried at 60 °C for 8 h.

Synthesis of amine-functionalized silica. Amine functionalization was done by adding APTES into a silica and ethanol mixture with a 1:0.5 (m/m) ratio of silica:APTES. After sonication for 2 h, the mixture was stirred for 6 h at room temperature. The filtrate and residue were then separated through centrifugation. Furthermore, the obtained filtrate was washed with ethanol and water three times and then dried at 60 °C for 12 h.

Immobilization of Ni(II). The SiO_2/Ni(II) catalyst was prepared using the impregnation method. About 0.9 g of $Ni(NO_3)_2{\cdot}6H_2O$ was dissolved in ethanol, and 1 g of SiO_2 was added to it. The resulting mixture was sonicated for 3 h at room temperature, filtered, and dried at 60 °C for 8 h. The same procedure was done for SiO_2/APTES/Ni(II) synthesis by substituting the SiO_2 with SiO_2/APTES.

General procedure for the acetylation of benzyl alcohol. Catalyst activity in the acetylation of benzyl alcohol was facilitated by ultrasonication treatment at 45 °C for 5 h. As much as 50 mg of catalyst was added to 0.3 mL of benzyl alcohol, followed by 0.3 mL of acetic anhydride. The mixture was then sonicated for 5 h at 45 °C. After the reaction was finished, the liquid mixture was quenched with distilled water, and ethyl acetate was used to extract the organic layer. The extracted organic layer was next washed with saturated Na_2CO_3 solution, brine, and water. Anhydrous sodium sulfate (Na_2SO_4) was utilized to dry the organic layer, and the remaining solvent was evaporated using a rotary evaporator. Benzyl acetate as the final product was then obtained and analyzed using GC.

Reusability test. The reusability of the catalyst was evaluated for the acetylation of benzyl alcohol under the same reaction conditions as described before. The catalyst regeneration was done by washing the used catalyst with distilled water and ethyl acetate. The washed catalyst was then heated in an oven for 6 h at 60 °C. Furthermore, the catalyst was added to the benzyl alcohol, followed by acetic anhydride. Afterward, the product separation was conducted by separating the organic layer, washing it with saturated Na_2CO_3 solution, brine solution, and water, and then drying with anhydrous sodium sulfate. The residual solvent was finally removed through evaporation. In this study, the catalyst was reused in three successive reaction cycles to determine its reusability.

Results and Discussion

Characterization of the synthesized catalyst. The diffraction pattern of the synthesized silica is depicted in Figure 1. The XRD peaks were indexed using ICDD files. A broad peak in the diffractogram indicates the amorphous phase of silica. According to ICDD code 00-029-0085, a peak broadening at 2θ around 22°–23° suggests the formation of amorphous silica. A similar result was reported by Dhaneswara *et al.* [19], who synthesized amorphous silica from rice husk ash using various concentrations of NaOH and acidification methods. This synthesis of silica through alkaline extraction results in entirely amorphous silica due to solubilization by sodium hydroxide, followed by precipitation [20].

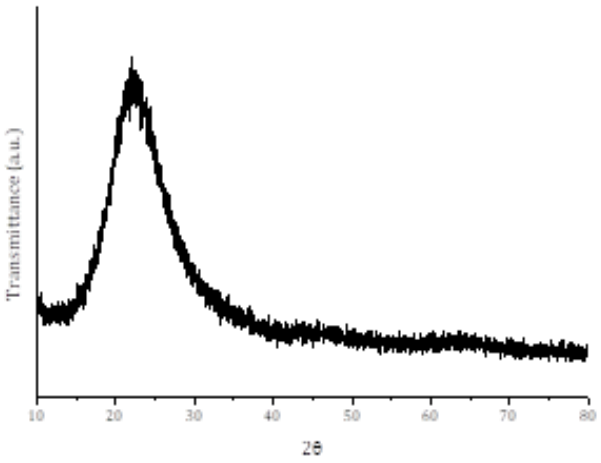

Figure 1. XRD Diffraction Pattern of Synthesized Silica

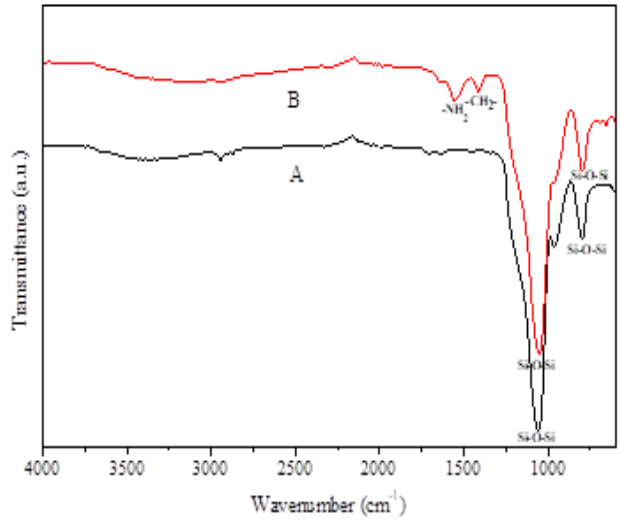

Figure 2. IR Spectra of SiO_2 Before (A) and After APTES Functionalization (B)

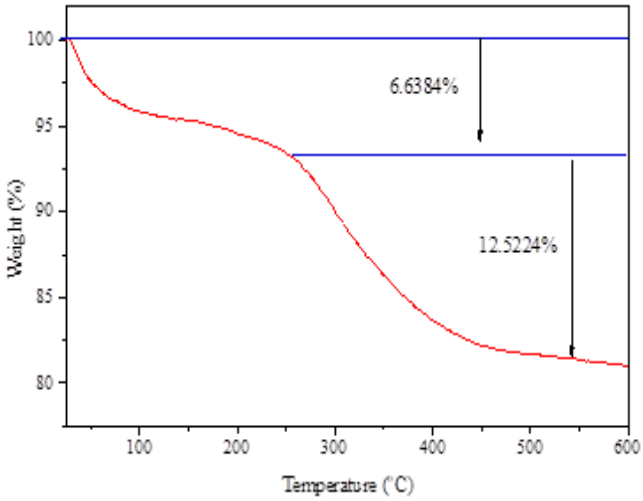

Figure 3. TGA Curve for SiO_2/APTES

Furthermore, the IR spectra in Figure 2 show the characteristic peaks of silica at 1,061 and 795 cm^{-1}, attributed to the asymmetric stretching vibration of siloxane bonds (Si–O–Si). The silica functionalization with APTES as an interparticle linker agent optimizes the interaction between silica and metal ion catalysts [21]. After amine functionalization, SiO_2/APTES exhibits an additional peak at 1,556 cm^{-1}, corresponding to the bending vibration of the $–NH_2$ group [22]. The appearance of these peaks confirms the presence of amine groups on the surface of functionalized silica. Additionally, the $–CH_2–$ bending vibration observed at 1,411 cm^{-1} confirms the successful addition of APTES to SiO_2.

The TGA curve of SiO_2/APTES in Figure 3 reveals two stages of decomposition that took place in SiO_2/APTES. The first stage occurred at 30 °C–50 °C with a mass loss percentage of 6.6384%. This mass loss in the given temperature range was attributed to the loss of physically adsorbed water on the surface of the catalyst. Another weight loss of 12.5224wt% resulted in the 200 °C–600 °C temperature range, corresponding to the condensation of silanol groups into siloxane, accompanied by the decomposition of the aliphatic carbon chains belonging to APTES [23]. Usgidaarachchi *et al*. [24] reported TGA curves of mesoporous silica nanoparticles in their works. The synthesized mesoporous silica exhibited excellent stability across the analyzed temperature range except in the initial one because of the presence of adsorbed water within the silica framework. A negligible mass loss was observed in the 100 °C–800 °C range, corresponding to the dihydroxylation and dehydration of the silica structure. However, in this study, significant weight loss at 200 °C–600 °C was obtained from the decomposition of the APTES carbon chain. The presence of aliphatic carbon chains on silica was validated by FTIR spectra.

As determined by atomic absorption spectroscopy results, the amounts of Ni(II) successfully immobilized on SiO_2 and SiO_2/APTES were 2.61 mmol (87%) and 2.81 mmol (94%), respectively. Functionalizing SiO_2 with amines through the addition of APTES enhanced the affinity of Ni^{2+} ions as the nitrogen from the amine group could interact with these divalent cations [25]. The interaction of SiO_2/APTES with Ni(II) occurred through an acid–base reaction between the amine groups in APTES and the metal ions. In this reaction, the amine group of APTES acted as a Lewis base, donating a lone pair of electrons to the vacant orbital belonging to the metal ion, which served as a Lewis acid [26]. Furthermore, the $–NH_2$ group peaks in the IR spectra of SiO_2/APTES/Ni shifted to 1,520 cm^{-1}. This change suggests the formation of a bond between N–H and Ni(II) [22]. Meanwhile, there was no significant change in the IR spectra of SiO_2 after Ni(II) immobilization, which indicated that Ni(II) was attached to the supporting material through physical interaction.

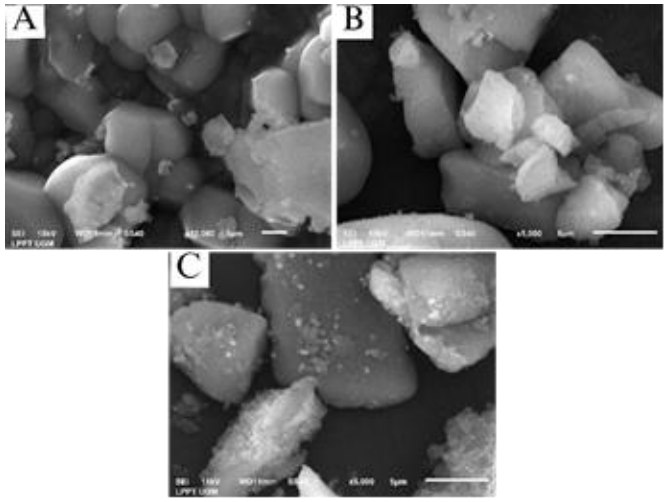

Figure 4. SEM Images of SiO_2 (A), SiO_2/Ni(II) (B), and SiO_2/APTES/Ni(II) (C)

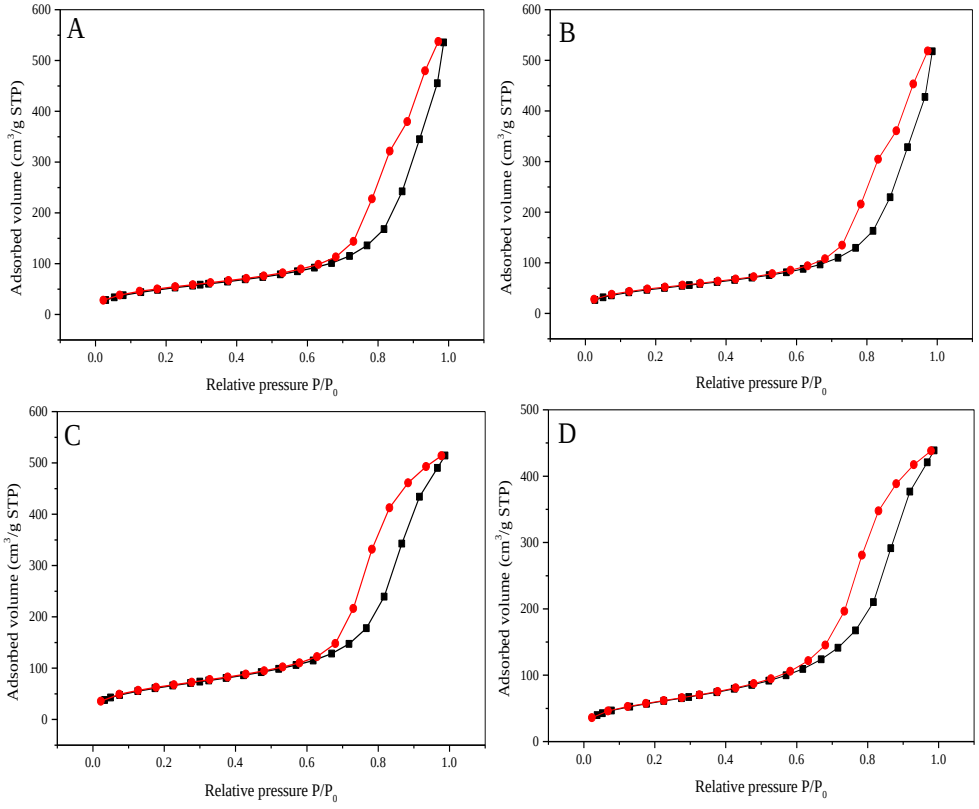

Figure 5. N_2 Adsorption–Desorption Isotherms of SiO_2 (A), SiO_2/Ni(II) (B), SiO_2/APTES (C), and SiO_2/APTES/Ni(II) (D)

Table 1. Physical Parameters of the Catalysts

Sample	S_{BET} (m^2/g)	V_p (cm^3/g)	D_p (nm)
SiO_2	184.28	0.83	17.68
SiO_2/ Ni(II)	177.18	0.66	14.71
SiO_2/APTES	238.64	0.79	13.61
SiO_2/APTES/Ni(II)	218.26	0.68	12.83

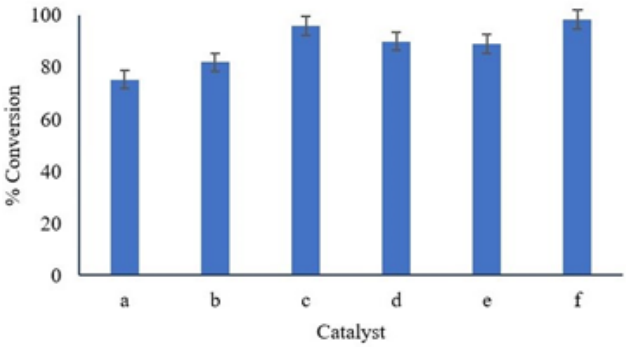

Figure 6. Conversion of Benzyl Alcohol (a. Noncatalyst; b. SiO_2; c. SiO_2/Ni(II); d. SiO_2/APTES; and e. SiO_2/APTES/Ni(II))

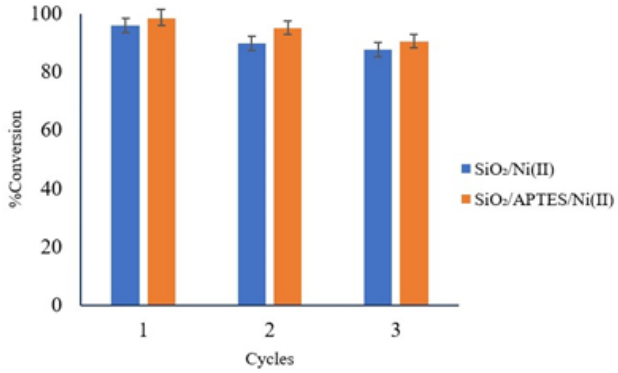

Figure 7. Benzyl Alcohol Conversion for Three Reaction Cycles from SiO_2/Ni(II) and SiO_2/APTES/Ni(II)

Figure 4 shows the SEM microphotographs of the studied materials after Ni(II) immobilization. The SEM micrographs in Figure 4a display the morphology of SiO_2 before amine functionalization and Ni(II) immobilization, showing a smooth surface. The surface of the silica became rough after Ni(II) addition, indicating the successful immobilization of Ni(II) on its surface. After amine functionalization, the surfaces of SiO_2 showed a greater degree of roughness compared with the unfunctionalized surface because of the presence of APTES, which enhanced the metal–support interaction, allowing more Ni(II) to disperse on the SiO_2/APTES surface [27].

The N_2 adsorption–desorption isotherm curves of SiO_2, SiO_2/Ni(II), SiO_2/APTES, and SiO_2/APTES/NI(II) are presented in Figure 5. According to the International Union of Pure and Applied Chemistry classification, all adsorption–desorption isotherms exhibited a type IV shape, indicating mesoporous materials based on Barrett–Joyner–Halenda adsorption. Table 1 provides the physical parameters of the catalysts, including total pore volume, average pore diameter, and specific surface area. The immobilization of Ni(II) affected the pore radii of the silica as a support material. The presence of Ni(II) on the catalyst reduced the average pore sizes and total pore volume because of the dispersion of Ni(II) both on the outer and inner surfaces of silica, leading to blocked silica pores [28]. Then, the APTES functionalization on silica changed the pore diameter of the catalyst material. The addition of APTES as a linker agent modified the silica surface because of the chemical bond between APTES and silica. The aminopropyl chain of APTES was assumed to be in a terminal position on the silica surface, obstructing the pores and reducing the measured pore size [15]. In contrast to SiO_2, the immobilization of Ni(II) on SiO_2/APTES did not significantly change the pore diameter of the materials as a result of the different interactions between Ni(II) and the supporting material. In SiO_2, the nickel ions interacted directly with the silica surface, whereas in SiO_2/APTES, they first attached to the nitrogen from the amines group, resulting in less noticeable effects on the silica pores.

Table 1 shows the differences in surface area after Ni(II) immobilization. The surface area of silica was diminished after nickel ion immobilization due to pore blockage. Meanwhile, the sample with amine functionalization created different trends. The surface area was enlarged after functionalization as the addition of APTES could increase the roughness of the silica surface, as shown in Figure 4. After nickel immobilization, the surface area was noticeably reduced because of the even dispersion of Ni and pore blockage.

Catalytic testing for acetylation of benzyl alcohol. The data in Figure 6 shows that the addition of SiO_2 catalyst enhanced the conversion of benzyl alcohol from 75.23% to 81.90%. This enhancement was attributed to the presence of acidic sites on silica, particularly hydroxyl groups on silanol groups catalyzing the acetylation of benzyl alcohol [29]. The APTES modification on silica further increased the yield of benzyl alcohol conversion by acting as a base catalyst in the acetylation reaction of benzyl alcohol with acetic anhydride [30]. The SiO_2/Ni(II) and SiO_2/APTES/Ni(II) catalysts yielded 98.34% and 95.97% conversion of benzyl alcohol, respectively. In addition, the catalyst with nickel immobilization exhibited a higher conversion of benzyl alcohol. During the acetylation of benzyl alcohol, the catalyst performance was significantly affected by the presence of dispersed Ni on the surface of the silica. The amine group of APTES optimized the immobilization of metal ions on the silica surface in the presence of nitrogenous base sites. The proposed mechanism for the acetylation of benzyl alcohol with the addition of SiO_2/Ni(II) and SiO_2/APTES/Ni(II) involved the coordination bond between Ni(II) and acetic anhydride to form an activated intermediate. Then, the carbonyl carbon of the activated intermediate was attacked by the hydroxyl group of the benzyl alcohol, forming a tetrahedral intermediate, followed by proton exchange via an acidic proton shift. Subsequently, another intermediate was formed by the elimination of acetic

acid, ultimately releasing the Ni(II) catalyst and benzyl acetate as the main product [31].

Reusability. The catalyst reusability was examined using catalyst regeneration between reaction cycles. After three cycles of acetylation, there was an insignificant change in catalyst activity, as shown in Figure 7. In the first cycle, the conversions of benzyl alcohol were 98.34% and 95.97% given by SiO_2/Ni(II) and SiO_2/Ni(II)/APTES, respectively. Then, there were slight decreases at 95.20% and 89.92% in the second cycle, respectively, followed by continued drops of 90.61% and 87.76% in the third one. These reductions in the catalytic performance of the catalyst material were likely due to two factors: a reduction in catalyst mass during the recycling process and the release of some metal ions from the surface of the catalyst after multiple uses. The APTES compound in SiO_2/APTES/Ni(II) contributed to binding Ni(II) ions more vigorously, thereby preventing these ions from being released during the reaction.

Conclusion

The results show that SiO_2/APTES/Ni(II) had greater activity than SiO_2/Ni(II) because of the higher content of Ni(II) in the catalyst functionalized by amine groups. This was caused by different interactions between Ni(II) with the supporting material. Whereas Ni(II) only had physical interaction with SiO_2, the amine functionalization in SiO_2/APTES led to Ni being anchored on the outside surface by chemical interaction with N of amine and enhanced the amount of Ni(II) that attached to the support material. This structure could improve Ni(II) dispersion and provide greater catalytic active sites. The SiO_2/APTES/Ni(II) catalyst simultaneously maintained high catalytic activity for the acetylation of benzyl alcohol in mild conditions. Thus, the synthesized mesoporous SiO_2/APTES is expected to become an alternative to support active metal species for catalysis reactions.

References

[1] Sadeq, Z.E, Al-Obaidi, N.S., Hammoodi, O.G., Abd, A.N., Al-Mahdawi, A.S. 2022. Benzyl acetate: A review on synthetic methods. Eurasian J. Phys. Chem. Math. 9: 28–36.

[2] Liu, S.H. 2014. Catalytic synthesis of benzyl acetate by diatomite supported waugh-type $(NH_4)_6[MnMo_9O_{32}]\cdot 8H_2O$. Appl. Mech. Mater. 483: 38–41, https://doi.org/10.4028/www.scientific.net/AMM.483.38.

[3] Masoud, S.-N., Tahereh, K., Samansa, H. 2005. Highly selective esterification of tert-butanol by acetic acid anhydride over alumina-supported $InCl_3$, $GaCl_3$, $FeCl_3$, $ZnCl_2$, $CuCl_2$, $NiCl_2$, $CoCl_2$ and $MnCl_2$ catalysts. J. Mol. Catal. A–Chem. 235(1–2): 150–153, https://doi.org/10.1016/j.molcata.2005.03.042.

[4] Sarkar, S.M., Rahman, M.L., Yusoff, M.M. 2015 Highly active thiol-functionalized SBA-15 supported palladium catalyst for Sonogashira and Suzuki-Miyaura cross-coupling reactions. RSC Adv. 5(2): 1295–1300, https://doi.org/10.1039/C4RA13322F.

[5] Ahmad, Y.H., Mohamed, A.T., Mahmoud, K.A., Aljaber, A.S., Al-Qaradawi, S.Y. 2019 Natural clay-supported palladium catalysts for methane oxidation reaction: Effect of alloying. RSC Adv. 9(56):32928–32935, https://doi.org/10.1039/C9RA06804J.

[6] Martins, A., Nunes, N., Carvalho, A.P., Martins, L.M.D.R.S. 2022. Zeolites and related materials as catalyst supports for hydrocarbon oxidation reactions. Catalysts. 12(2): 154, https://doi.org/10.3390/catal12020154.

[7] Miao, C., Cai, L., Wang, Y., Xu, X., Yang, J., He, Y., *et al*. 2021. Array modified molded alumina supported PdAg catalyst for selective acetylene hydrogenation: Intrinsic kinetics enhancement and thermal effect optimization. Ind. Eng. Chem. Res. 60(23): 8362–8374, https://doi.org/10.1021/acs.iecr.1c00423.

[8] Manjare, S.B., Chaudhari, R.A., Thopate, S.R., Risbud, K.P., Badade, S.M. 2020 Resin loaded palladium nanoparticle catalyst, characterization and application in –C–C– coupling reaction. SN Appl. Sci. 2: 988, https://doi.org/10.1007/s42452-020-2795-z.

[9] Alam, M., Rahman, A., Alandis, N., Shaik, M.R. 2013. Report on selective acylation of benylic alcohol to benzyl acetate with catalytic system Ni/SiO2 : An environmentally benevolent approach. Oxid. Commun. 36(1): 261–270.

[10] Setyawan, N., Hoerudin, Yuliani, S. 2021. Synthesis of silica from rice husk by sol-gel method. IOP Conf. Ser. Earth Environ. Sci. 733: 012149, https://dx.doi.org/10.1088/1755-1315/733/1/012149.

[11] Demirörs, A.F., Van Blaaderen, A., Imhof, A. 2009 Synthesis of eccentric titania-silica core-shell and composite particles. Chem. Mater. 21(6): 979–984, https://doi.org/10.1021/cm803250w.

[12] Guenther, J., Reibenspies, J., Blümel, J. 2019. Synthesis and characterization of tridentate phosphine ligands incorporating long methylene chains and ethoxysilane groups for immobilizing molecular rhodium catalysts. Mol. Catal. 479: 110629, https://doi.org/10.1016/j.mcat.2019.110629.

[13] Arrozi, U.S.F., Bon, V., Krause, S., Lübken, T., Weiss, M.S., Senkovska, I., *et al*. 2020. *In situ* imine-based linker formation for the synthesis of zirconium MOFs: A route to CO_2 capture materials and ethylene oligomerization catalysts. Inorg. Chem. 59(1): 350–359, https://doi.org/10.1021/acs.inorgchem.9b02517.

[14] Sharma, H., Mahajan, H., Jamwal, B., Paul, S. 2018. Cu@Fe_3O_4-TiO_2-L-dopa: A novel and magnetic

catalyst for the Chan-Lam cross-coupling reaction in ligand free conditions. Catal. Commun. 107: 68–73, https://doi.org/10.1016/j.catcom.2018.01.016.

[15] Jamwal, B., Kaur, M., Sharma, H., Khajuria, C., Paul, S., Clark, J.H. 2019. Diamines as interparticle linkers for silica-titania supported PdCu bimetallic nanoparticles in Chan-Lam and Suzuki cross-coupling reactions. New J. Chem. 43(12): 4919–4928, https://doi.org/10.1039/C8NJ05050C.

[16] Agustiningsih, D., Nuryono, N., Santosa, S.J., Kunarti, E.S. 2023. Propylamine silica-titania hybrid material modified with Ni(II) as the catalyst for benzyl alcohol to benzaldehyde conversion. Indones. J. Chem. 23(5): 1361–1374, https://doi.org/10.22146/ijc.84282.

[17] Agustiningsih, D., Otomo, R., Kamiya, Y., Nuryono, N., Santosa, S.J., Kunarti, E.S. 2024. Fixing Ni^{2+} onto mesoporous SiO_2-TiO_2 through amino silane and application as a catalyst for Kumada cross coupling reaction for 1,1′-biphenyl synthesis. Appl. Catal. A-Gen. 672: 119606, https://doi.org/10.1016/j.apcata.2024.119606.

[18] Widiyandari, H., Pardoyo, P., Sartika, J., Putra, O. A., Purwanto, A., Ernawati, L. 2021. Synthesis of Mesoporous Silica Xerogel from Geothermal Sludge using Sulfuric Acid as Gelation Agent. Int. J. Eng. Trans. A Basics. 34(7): 1569–1575, https://doi.org/10.5829/IJE.2021.34.07A.02.

[19] Dhaneswara, D., Fatriansyah, J.F., Situmorang, F.W., Nurul, A. 2020. Synthesis of amorphous silica from rice husk ash: Comparing HCl and CH_3COOH acidification methods and various alkaline concentrations. Int. J. Technol. 11(1): 200–208, https://doi.org/10.14716/ijtech.v11i1.3335.

[20] Fernandes, I.J., Calheiro, D., Sánchez, F.A.L., Camacho, A.L.D., Rocha, T.L.A.D.C., Moraes, C.A.M., *et al*. 2017. Characterization of silica produced from rice husk ash: Comparison of purification and processing methods. Mater. Res. 20(Suppl 2): 519–525, https://doi.org/10.1590/1980-5373-MR-2016-1043.

[21] Xia, W. 2016. Interactions between metal species and nitrogen-functionalized carbon nanotubes. Catal. Sci. Technol. 6(3): 630–644, https://doi.org/10.1039/C5CY01694K.

[22] Mandal, P., Molla, R.A., Chattopadhyay, A.P., Poddar, S., Biswas, H.S. 2022. GO-APTES-Cu (II) Schiff base complex as efficient heterogeneous catalyst for aerobic decarboxylation reaction of phenylacetic acids. Inorg. Chem. Commun. 144: 109825, https://doi.org/10.1016/j.inoche.2022.109825.

[23] Cueto-Díaz, E.J., Castro-Muñiz, A., Suárez-García, F., Gálvez-Martínez, S., Torquemada-Vico, M.C., Valles-González, M.P., *et al*. 2021. APTES-based silica nanoparticles as a potential modifier for the selective sequestration of CO_2 gas molecules. Nanomaterials. 11(11): 2893, https://doi.org/10.3390/nano11112893.

[24] Usgodaarachchi, L., Thambiliyagodage, C., Wijesekera, R., Bakker, M.G. 2021. Current research in green and sustainable chemistry synthesis of mesoporous silica nanoparticles derived from rice husk and surface-controlled amine functionalization for efficient adsorption of methylene blue from aqueous solution. Curr. Res. Green Sustain. Chem. 4: 100116, https://doi.org/10.1016/j.crgsc.2021.100116.

[25] Isasi, J., Arevalo, P., Martin, E., Martín-Hernández, F. 2019. Preparation and study of silica and APTES–silica-modified $NiFe_2O_4$ nanocomposites for removal of Cu^{2+} and Zn^{2+} ions from aqueous solutions. J. Sol-Gel Sci. Technol. 91: 596–610, https://doi.org/10.1007/s10971-019-05067-3.

[26] Smith, M.B. 2016. Organic Chemistry: An Acid-Base Approach, 2nd ed. CRC PRess. Boca Raton. pp 31–32.

[27] Liu, J., Hao, J., Hu, C., He, B., Xi, J., Xiao, J., *et al*. 2018. Palladium nanoparticles anchored on amine-functionalized silica nanotubes as a highly effective catalyst. J. Phys. Chem. C. 122(5): 2696-2703, https://doi.org/10.1021/acs.jpcc.7b10237.

[28] Budiman, A.W., Qurrotul'aini, N.'A, Latifah, N., Dewani, P.H., Rachmadhani, S., Wigati, S.M. 2022. The effects of different nickel–ruthenium on SiO_2 catalyst synthesis methods toward catalytic activity of methane dry reforming. Equilib. J. Chem. Eng. 5(2): 67–74, http://dx.doi.org/10.20961/equilibrium.v5i2.55175.

[29] Kusumaningtyas, D.T., Prasetyoko, D., Suprapto, S., Triwahyono, S., Jalil, A.A., Rosidah, A. 2017. Esterification of benzyl alcohol with acetic acid over mesoporous H-ZSM-5. Bull. Chem. React. Eng. Catal. 12(2): 243–250, https://doi.org/10.9767/bcrec.12.2.806.243-250.

[30] Vries, A.J.O.-d., Nieuwland, P.J., Bart, J., Koch, K., Janssen, J.W.G., van Bentum, P.J.M., *et al*. 2019. Inline reaction monitoring of amine-catalyzed acetylation of benzyl alcohol using a microfluidic stripline nuclear magnetic resonance setup. J. Am. Chem. Soc. 141(13): 5369–5380, https://doi.org/10.1021/jacs.9b00039.

[31] Sonawane, R.B., Sonawane, S.R., Rasal, N.K., Jagtap, S.V. 2020. Chemoselective: O-formyl and O-acyl protection of alkanolamines, phenoxyethanols and alcohols catalyzed by nickel(II) and copper(II)-catalysts. Green Chem. 22(10): 3186–3195, https://doi.org/10.1039/D0GC00520G.